Spartacus: A review and aggregation of reference datasets reporting the normal shoulder girdle kinematics during uniplanar humerus motions

Florent Moissenet, Pierre Puchaud, Alexandre Naaim, Nicolas Holzer, Mickaël Begon

Journal of Biomechanics 189 (2025) 112642

Contents lists available at ScienceDirect

Journal of Biomechanics

journal homepage: www.elsevier.com/locate/jbiomech

Review

Spartacus: A review and aggregation of reference datasets reporting the normal shoulder girdle kinematics during uniplanar humerus motions

Florent Moissenet [a,b,*,1], Pierre Puchaud [c,d,1], Alexandre Naaim [e], Nicolas Holzer [b,f], Mickaël Begon [c,d]

[a] Kinesiology Laboratory, Geneva University Hospitals and University of Geneva, Geneva, Switzerland
[b] Biomechanics Laboratory, Geneva University Hospitals and University of Geneva, Geneva, Switzerland
[c] Laboratoire de Simulation et Modélisation du Mouvement, École de Kinésiologie et des Sciences de l'Activité Physique, Faculté de Médecine, Université de Montréal, Montréal, Canada
[d] Centre de recherche Azrieli du CHU Sainte-Justine, Montréal, Canada
[e] Univ Lyon, Université Claude Bernard Lyon 1, Univ Gustave Eiffel, LBMC UMR_T9406, Lyon, France
[f] Orthopedic Surgery and Musculoskeletal Trauma Care Division, Department of Surgery, Geneva University Hospitals, Geneva, Switzerland

ARTICLE INFO

Keywords:
Shoulder kinematics
Scapulohumeral rhythm
Gold-standard
Open source
Open science
ISB Recommendations

ABSTRACT

Understanding 3D shoulder girdle kinematics is essential for applications in medicine, sports, and computational biomechanics, where reference data help quantify deviations from the standard. Unfortunately, existing datasets on shoulder kinematics based on gold-standard measurements are often inconsistent in data collection methods, segment definitions, and joint kinematics computation, limiting their relevance. This study reviews and aggregates available datasets to establish Spartacus, a comprehensive reference for normal shoulder girdle kinematics. We gathered 20 datasets, published between 2000 and 2023, and aligned them, when possible, with the International Society of Biomechanics recommendations to enable population-wide analysis. Spartacus comprises data recorded *in vivo* (70 %) or ex vivo (30 %) on 245 shoulders using intracortical pins (55 %) or imaging (45 %), primarily during active dynamic (65 %) movements. The dataset predominantly covers arm elevation records in the scapular (70 %), frontal (50 %), and sagittal (50 %) planes, but also includes internal-external rotation and horizontal flexion. Both rotations and translations are represented across all shoulder girdle joints, with scapulothoracic rotations being the most frequent (75 %). Our approach corrects or at least compensates for six identified deviations in local coordinate system definitions and joint kinematics computation methods. Substantial inconsistencies across existing datasets reveal a need for improved standardisation to facilitate reliable data comparisons. Spartacus, openly available, will enable researchers to explore normal shoulder girdle kinematics, and provides a foundation for future clinical and biomechanical studies.

1. Introduction

The shoulder girdle is the joint complex with the greatest range of motion in the human body. It includes four joints: the sternoclavicular, acromioclavicular, scapulothoracic, and glenohumeral joints. The 3D kinematic analysis of the shoulder girdle is of significant interest in many fields. In medicine, shoulder kinematics can be a distinctive feature of joint disorders and thus plays a key role in diagnosis, treatment follow-up, and assessment of outcomes (Longo et al., 2022). Kinematics can also guide the design of orthopaedic implants and the selection of their geometry and setup by means of surgical planning and simulation software (Como et al., 2022). In sport, shoulder kinematics is related to the athlete's performance and to the prevention of injuries (Cools et al., 2021). In computational biomechanics, shoulder kinematics is often required to verify measurement methods affected by soft tissue artefacts (e.g., marker-based or markerless motion capture and inertial measurement units) (Blache et al., 2017), and to design and validate upper-limb multibody models (Duprey et al., 2017). Across these diverse applications, a comprehensive reference dataset for the normal (i.e., asymptomatic) shoulder girdle remains unavailable, limiting comparative analyses and methodological validations.

Intracortical pins, x-ray radiography, CT-scan, and MRI allow for true

* Corresponding author at: Laboratoire de Cinésiologie, HUG, 4 rue Gabrielle-Perret-Gentil, CH-1211 Geneva 14, Switzerland.
E-mail address: florent.moissenet@unige.ch (F. Moissenet).
[1] Authors' equal contribution to the manuscript.

https://doi.org/10.1016/j.jbiomech.2025.112642
Accepted 24 March 2025
Available online 27 March 2025

joint kinematic measurements (i.e., free of soft tissue artefacts) and are recognised as gold-standard measurement methods (Cereatti et al., 2017). However, these methods often raise ethical and experimental challenges, limiting the number of extensive data collections. Nonetheless, over the years, some noteworthy studies have reported gold-standard shoulder girdle joint kinematics. However, no comprehensive inventory currently exists. The information provided by these studies with highly valuable data is often partial, stemming from their limitations in the examined joints and reported degrees-of-freedom (DoF), the variety of motor tasks, and the sample size. A structured aggregation of these studies could bridge these gaps, creating a unified, high-quality dataset that enhances our understanding of shoulder biomechanics, facilitates the validation of alternative measurement methods, and strengthens applications in medicine, sports, and computational modelling.

The first objective of this study was to perform a literature review and aggregation of available datasets reporting the 3D kinematics of the normal shoulder girdle using gold-standard measurement methods. This review was intentionally restricted to uniplanar humerus motions because other motions such as activities of daily life typically involve humeral movement across multiple thoracic planes simultaneously. As a result, describing the shoulder rhythm as a function of a single thoracohumeral angle is not feasible. Specifically, an open dataset (called Spartacus) is made available to the community. To aggregate datasets effectively, a consistent convention must be applied across all measurements to merge and compare them. The ISB recommendations (Wu et al., 2005), which served for the past two decades as a reference to report joint kinematics, were used here for that purpose. These recommendations include 1) the definition of local coordinate systems (LCS) (i.e., axes' orientations, axes' directions, and origin) and 2) a computational approach aiming to express joint rotations using Euler angles and joint translations along proximal LCS axes. Nevertheless, it was expected that some datasets did not entirely satisfy the ISB recommendations. Thus, the second objective of this study was to highlight discrepancies among the original datasets and assess their compliance with the ISB recommendations. The resulting observations illustrate the current application trends of the ISB recommendations. The last objective of this study was to apply, where possible, a methodology aimed at correcting or at least compensating for these deviations. To the best of our knowledge, only Gasparutto et al. (2017) and Ortigas Vásquez et al. (2023) proposed such methods, although they have been applied exclusively to knee kinematics. Another method proposed by Kolz et al. (2020) compensates for deviations on scapula LCS axes' directions but has never been applied to compare existing datasets yet.

2. Methods

2.1. Review and aggregation of original datasets

Original sources were identified in the current literature (until December 2023) through a search in the Embase, Medline, Scopus, and Web of Science databases. Several combinations of the following keywords in the title, abstract, or keywords were used to this end through a citation snowballing procedure. These keywords were identified using the PICO process (Nishikawa-Pacher, 2022): *'healthy', 'normal', 'asymptomatic', 'cadaver*', 'in vivo', 'ex vivo', 'xray', 'fluoroscop*', 'MRI', '4DCT', 'imaging', 'pins', 'shoulder', 'glenohumeral', 'scapulothoracic', 'acromioclavicular', 'sternoclavicular', 'shoulder girdle', 'joint', 'kinemat*', 'motion', 'movement','rotation', 'translation', 'displacement'*. As kinematic series (i.e., angle-angle or translation-angle data series measured in discrete increments, but not as a function of time such as angle-time data series) reported as curves were the primary outcomes of the present study, conventional standards for reporting systematic reviews (i.e., the Preferred Reporting Items for Systematic review and Meta-Analysis (PRISMA) statement (Moher et al., 2009)) were not suitable nor used here.

Resulting sources were screened by three authors (FM, PP, and AN) to check their eligibility and cross-referenced. Inclusion criteria were 1) to report kinematic data related to at least one rotational or translational DoF of the shoulder girdle, 2) collected *in vivo* or *ex vivo* from an asymptomatic population, 3) using a gold-standard measurement method, 4) during at least one uniplanar humerus motion (i.e., frontal, scapular, and sagittal plane elevations, internal-external rotations at 0° and 90° of frontal plane elevation, and horizontal flexion), and 5) reported as continuous variables using kinematic series that were 6) expressed as a function of a thoracohumeral angle. *Ex vivo* experiments were included not only to enlarge the dataset but also to provide insights into the scapulohumeral rhythm without muscle activation. Studies reporting kinematic series expressed as a function of the glenohumeral angle were excluded, as the thoracohumeral angle was preferred. Indeed, the thoracohumeral angle provides a more comprehensive representation of shoulder complex movement and ensures consistency in biomechanical and clinical analyses (Kontaxis et al., 2009).

All authors were contacted to obtain original data and clarify experimental and computational choices. When the authors and/or data were unavailable, kinematic series were digitised using a manual point and axis matching approach in the Engauge Digitizer software (12.1) (Mitchell et al., 2020). The data were grouped into datasets if they came from measurements carried out by the same group on the same participants, during the same recording session, using the same experimental protocol. Seventy-six features were extracted for each dataset about the source (e.g., authors, date, doi), participants (e.g., *in vivo* or *ex vivo*, sample size), measurement tools (e.g., intracortical pins, biplane x-ray fluoroscopy), experimental procedure (e.g., participants posture, humerus motions), segment LCS (e.g., origin, X-Y-Z axis definitions), joint definitions (e.g., parent body, related Euler sequence), and available kinematic series (e.g., related DoFs).

2.2. Identification of deviations from ISB recommendations

As stated in the Introduction, the ISB recommendations (see Supplementary material 1) were chosen as a reference for defining the LCS as well as for computing joint kinematics.

Six deviations from the ISB recommendations were identified (Table 2). The first deviation (D1) refers to the orientation of the LCS axes for a bony segment (e.g., $\mathbf{X}_{scapula}$ not following the anteroposterior direction and/or pointing posteriorly). The second deviation (D2) is about the construction method of at least one LCS axis, either using incorrect ISB landmarks or non-ISB landmarks (e.g., $\mathbf{Z}_{scapula}$ not constructed using the acromial angle and the trigonum spinae landmarks). The third deviation (D3) concerns the LCS origin of a bony segment. The fourth deviation (D4) corresponds to the Euler sequence used to express joint rotations. The fifth deviation (D5) corresponds to the coordinate system used to express joint translations. The sixth deviation (D6) corresponds to the thoracohumeral joint angle computation describing humerus motion. This last deviation is not recommended by the ISB, but states as a common practice allowing data comparison whatever the observed range of motion (Haering et al., 2014).

These deviations were identified from dataset features using a Python package (Moissenet et al., 2025) and summarised at both segment level (i.e., deviations D1, D2, D3) and joint level (i.e., D4, D5, D6), using Circos link plots (Krzywinski et al., 2009). A compliance score was given for each joint of each dataset. For both rotations and translations, six deviations were chosen from the complete set of nine, spanning the parent segment, child segment, and the joint, as documented further in

Supplementary material 2. The resulting compliance scores were expressed as a percentage, where 100 % corresponds to a dataset applying strictly the ISB recommendations.

2.3. Correcting or compensating for deviations from the ISB recommendations

Depending on the deviation and available methods, deviations from the ISB recommendations were corrected or compensated. Deviation *correction* stands for the complete removal of the deviation, aiming to nullify/rectify its impact on the data. Deviation *compensation* stands for the partial correction of the deviation, reducing its effect on the data without eliminating it entirely. Left shoulder data were converted to right shoulder data, see the Appendix.

Deviations in LCS axes' orientation (D1) were corrected by applying a rotation matrix ${}^{S_{ISB_0}}\mathbf{R}_S$, which adjusted the LCS axes' orientation of the segment S (that can be distal D or proximal P) with an intermediate ISB-oriented frame. For that, a parsing method was developed to compute biomechanical directions based on reported anatomical landmarks. A specific terminology was chosen to ensure that each axis points in the correct direction, even if it does not strictly adhere to ISB recommendations for axis orientation (see deviation D2). For the right side and whatever the body segment, **X** was defined + posteroanterior (pointing anteriorly), **Y** was defined + inferosuperior (pointing superiorly), and **Z** was defined + mediolateral (pointing laterally).

Correcting deviations in LCS axes' direction (D2) requires the coordinates of the relevant ISB anatomical landmarks. When not available, a compensation approach was only possible for the scapula LCS, as Kolz et al. (2020) provided averaged rotation matrices ${}^{S_{ISB}}\mathbf{R}_{S_{ISB_0}}$ to facilitate switching from several non-ISB LCS to the ISB LCS (when the averaged rotation matrix was unavailable, this transformation defaulted to the identity matrix). To summarise, deviations in LCS axes' orientation (D1) and direction (D2) were corrected or compensated using the following formula (1):

$$ {}^{P_{ISB}}\mathbf{R}_{D_{ISB}} = \underbrace{{}^{P_{ISB}}\mathbf{R}_{P_{ISB_0}}}_{\substack{proximal\\ D2\ correction\\ or\ compensation}} \cdot \underbrace{{}^{P_{ISB_0}}\mathbf{R}_P}_{\substack{proximal\\ D1\ correction}} \cdot {}^{P}\mathbf{R}_D \cdot \underbrace{\left({}^{D_{ISB_0}}\mathbf{R}_D\right)^{\mathrm{T}}}_{\substack{distal\\ D1\ correction}} \cdot \underbrace{\left({}^{D_{ISB_0}}\mathbf{R}_{D_{ISB}}\right)^{\mathrm{T}}}_{\substack{distal\\ D2\ correction\\ or\ compensation}} \quad (1) $$

where ${}^{P}\mathbf{R}_D$ represents the original transformation from the proximal to the distal LCS as constructed from the original dataset, while ${}^{P_{ISB}}\mathbf{R}_{D_{ISB}}$ is the transformation from the proximal to the distal LCS that strictly adheres to ISB recommendations, when possible. Joint kinematics was extracted from ${}^{P_{ISB}}\mathbf{R}_{D_{ISB}}$. Correcting deviations in LCS origin (D3) requires the coordinates of the relevant ISB anatomical landmarks. When not available, these deviations were not corrected nor compensated. Deviations in Euler sequence (D4) were corrected by computing joint angles from the resulting rotation matrix ${}^{P_{ISB}}\mathbf{R}_{D_{ISB}}$ using the ISB-recommended Euler sequence.

Deviations in translations' coordinate system (D5) were corrected by adapting previous transformations to express the translation from proximal to distal segment in the proximal LCS as follows:

$$ {}^{P_{ISB}}\mathbf{t}_{D_{ISB}} = {}^{P_{ISB}}\mathbf{R}_{P_{ISB_0}} \cdot \mathrm{diag}(1, 1, -1 \text{ or } 1)^{\mathrm{T}} \cdot {}^{P_{ISB_0}}\mathbf{R}_P \cdot {}^{P}\mathbf{t}_D \quad (2) $$

where ${}^{P}\mathbf{t}_D$ represents the translation of the distal segment from the original proximal LCS, while ${}^{P_{ISB}}\mathbf{t}_{D_{ISB}}$ adheres to the ISB recommendations, when possible.

Correcting deviations in thoracohumeral joint angle (D6) requires the rotation matrices for the thoracohumeral joint to reinterpret angles. When not available, these deviations were not corrected nor compensated.

3. Results

3.1. Aggregation of original datasets

The search strategy allowed us to identify 20 datasets from 30 original sources (peer-reviewed original papers, theses, conference proceedings). In most cases, the authors answered our emailed questions (18 out of 20, 90 %), and original data were obtained in half the cases (10 out of 20) while other original data was no longer available. The aggregation of original datasets with their 76 features is available to the community through an open dataset, called Spartacus, freely available (Moissenet et al., 2025).

The primary features of the original datasets are reported in Table 1. Datasets have been published regularly over the last two decades (from 2000 to 2023). They are composed of a large variety in terms of experimental conditions, measurement methods, movement types, uniplanar humerus motions, and reported degrees of freedom (Fig. 1). Demographic data when available were gathered in the Supplementary Material 5.

3.2. Reporting of identified deviations from the ISB recommendations

Despite the ISB recommendations, the original datasets exhibited a considerable variety of LCS for each bony segment: 8 for the thorax, 8 for the clavicle, 11 for the scapula, and 8 for the humerus (Fig. 2). All these LCS have been synthetised, including details on axis construction (see Supplementary material 3 and Moissenet et al., 2025).

While 85 % (17 out of 20) of the included datasets are related to original sources published after the ISB recommendations for upper limb segment and joint coordinate systems (Wu et al., 2005) (i.e., after 2005), numerous occurrences of the six reported deviations from the ISB recommendations are observed (Table 2, Fig. 3), with a prevalence of deviations occurring at the segment level (61 %).

At the segment level (deviations D1, D2, and D3), the ISB recommendations were fully respected in only 35 % of cases for the thorax (7 out of 20), 22 % for the clavicle (2 out of 9), 35 % for the scapula (7 out of 20), and 42 % for the humerus (8 out of 19). It must be noted that two types of LCS were observed for the scapula, segment-based LCS defining the overall bony segment, and joint-based LCS focusing on the glenoid, i.e., the articular surface. Interestingly, 60 % (6 out of 10) imaging-based datasets used joint-based LCS. At the joint level, by cumulating proximal LCS deviations, distal LCS deviations, and joint-related deviations (D4, D5, and D6), the ISB recommendations were fully respected in only 25 % of cases for the sternoclavicular joint (2 out of 8), 0 % for the acromioclavicular joint (0 out of 5), 33 % for the scapulothoracic joint (5 out of 15), and 10 % for the glenohumeral joint (1 out of 10).

This results in various compliance scores with the ISB recommendations across joints and original datasets, for both rotations and translations (Fig. 4). Only 15 % (3 out of 20) of the original datasets demonstrated a median compliance score across all DoFs of 100 %. On average, the compliance scores were high for the sternoclavicular translations (83 %, but with the lowest related number of original datasets), medium for glenohumeral rotations (67 %), and low or very low for all other DoFs.

3.3. Correcting or compensating for deviations from the ISB recommendations

Correction of the deviations in LCS axes' orientation (D1) resulted in 39 adjustments distributed across 12 datasets (#1, #2, #4, #7, #8, #9, #10, #12, #15, #17, #18, #19). As the coordinates of the relevant ISB anatomical landmarks were not made available except in 2 datasets (#6, #14), correction of the deviations in LCS axes' direction (D2) and in LCS origin (D3) were not corrected. Compensation of the deviations in LCS axes' direction (D2) resulted in 13 adjustments distributed across 3

Table 1
Primary features of the original datasets listed in alphabetical order by author.

ID	Authors[1]	Year[2]	Sources	Data type	Experimental conditions	Gold-standard measurement method	Sample size (shoulders)	Type of movement	Uniplanar humerus motions
#1	Begon et al.	2014	Blache and Begon, 2018; Dal Maso et al., 2014	Original	*In vivo*	Intracortical pins	2	Active dynamic	FRE, SAE, IER-0°, IER-90°
#2	Bourne et al.	2003	Bourne, 2009; Bourne et al., 2007	Digitised	*In vivo*	Intracortical pins	7	Active dynamic	FRE, HFL
#3	Chu et al.	2012	Chu et al., 2012	Digitised	*In vivo*	Biplane x-ray fluoroscopy	5	Active dynamic	FRE, SCE, IER-90°
#4	Fung et al.	2001	Fung et al., 2001	Original	*Ex vivo*	Intracortical pins	5	Passive dynamic	FRE, SCE, SAE
#5	Gutierrez Delgado et al.	2017	Gutierrez Delgado et al., 2017	Original	*Ex vivo*	Intracortical pins	1	Passive dynamic	FRE, SAE
#6a, #6b, #6c[3]	Henninger et al.	2020	Aliaj et al., 2022, 2021; Kolz et al., 2021, 2020	Original	*In vivo*	Biplane x-ray fluoroscopy	20	Active dynamic	FRE, SCE, SAE, IER-0°, IER-90°
#7	Karduna et al.	2000	Karduna et al., 2000; McClure et al., 2001	Original	*In vivo*	Intracortical pins	8	Active dynamic	SCE, SAE, IER-90°
#8	Kijima et al.	2015	Kijima et al., 2015	Digitised	*In vivo*	Single-plane x-ray fluoroscopy	7	Active dynamic	SCE
#9	Kim et al.	2017	Kim et al., 2017	Digitised	*In vivo*	Single-plane x-ray fluoroscopy	15	Active dynamic	SCE
#10	Kozono et al.	2017	Kozono et al., 2017	Digitised	*In vivo*	Single-plane x-ray fluoroscopy	10	Active dynamic	SCE, IER-0°
#11	Ludewig et al.	2009	Lawrence et al., 2014; Ludewig et al., 2009	Original	*In vivo*	Intracortical pins	12	Active dynamic	FRE, SCE, SAE
#12	Matsuki et al.	2011	Matsuki et al., 2014, 2012, 2011	Original	*In vivo*	Single-plane x-ray fluoroscopy	24	Active dynamic	SCE
#13	Matsumura et al.	2013	Matsumura et al., 2013	Digitised	*Ex vivo*	Intracortical pins	14	Passive dynamic	FRE, SCE, SAE
#14	Moissenet et al.	2023	Moissenet, 2023; Moissenet et al., 2023	Original	*Ex vivo*	Intracortical pins	10	Passive dynamic	SCE, SAE, HFL, IER-0°
#15	Nishinaka et al.	2008	Nishinaka et al., 2008	Digitised	*In vivo*	Single-plane x-ray fluoroscopy	9	Active dynamic	SCE
#16	Oki et al.	2012	Oki et al., 2012	Digitised	*Ex vivo*	Intracortical pins	14	Passive dynamic	FRE, SAE, HFL
#17	Sahara et al.	2006	Sahara et al., 2007, 2006	Digitised	*In vivo*	MRI	14	Active quasi-static	FRE
#18	Sugi et al.	2021	Sugi et al., 2021	Original	*In vivo*	Single-plane x-ray fluoroscopy	35	Active dynamic	SCE
#19	Teece et al.	2008	Teece et al., 2008	Digitised	*Ex vivo*	Intracortical pins	13	Passive dynamic	SCE
#20	Yoshida et al.	2023	Yoshida et al., 2023	Original	*In vivo*	4DCT	20	Active dynamic	SAE

FRE: Frontal plane elevation; HFL: Horizontal flexion; IER-0°: Internal-external rotation at 0° of frontal plane elevation; IER-90°: Internal-external rotation at 90° of frontal plane elevation; SAE: Sagittal plane elevation; SCE: Scapular plane elevation.

[1] When the dataset was linked to a single source or multiple sources with the same first author, the first author's name was reported. When the dataset was linked to multiple sources with various first authors, the more representative author's name was reported.

[2] In case of multiple sources, the year related to the first publication is reported.

[3] The dataset from Henninger et al. is available with three versions of the scapula local coordinate system: #6a follows ISB recommendations, #6b uses inferior angle, most dorsal point on the acromioclavicular joint, and trigonum spinae landmarks, and #6c uses inferior angle, glenoid centre, and trigonum spinae landmarks. However, datasets #6b and #6c are only provided in Spartacus for comparison purposes and were not considered in the present analyses.

datasets (#7, #11, #19). Correction of the deviations in Euler sequence (D4) and translations' coordinate system (D5) resulted in 16 corrections distributed across 9 datasets (#4, #8, #9, #10, #11, #12, #17, #18, #20) and 117 corrections distributed across 1 dataset (#14). As the rotation matrices for the thoracohumeral joint to reinterpret angles were not made available except in 3 datasets (#1, #6, #14), the deviations in thoracohumeral joint angle (D6) were not corrected.

The corrected datasets (where applicable) were used to generate kinematic series data that represent normal shoulder girdle kinematics during uniplanar humerus motions. All kinematic series can be explored through interactive charts (Moissenet et al., 2025). Users can filter the plotted kinematic series by joint, uniplanar humerus motions, and compliance score. An example is available in Fig. 5 concerning the scapulothoracic joint rotations during frontal, sagittal, and scapular plane elevations.

4. Discussion

The first aim of this study was to conduct a literature review and aggregation of available datasets reporting the 3D kinematics of the normal shoulder girdle during uniplanar humerus motions using gold-standard measurement methods. The second aim was to highlight discrepancies among the original datasets by assessing their compliance with the ISB recommendations. The third aim was to develop a methodology to correct or at least compensate for these discrepancies before aggregation.

We found that existing datasets are individually either too sparse or have sample sizes too small to support a comprehensive, population-wide analysis of normal shoulder girdle kinematics. Significant discrepancies were found across the original datasets, with limited compliance with the ISB recommendations, making direct comparisons

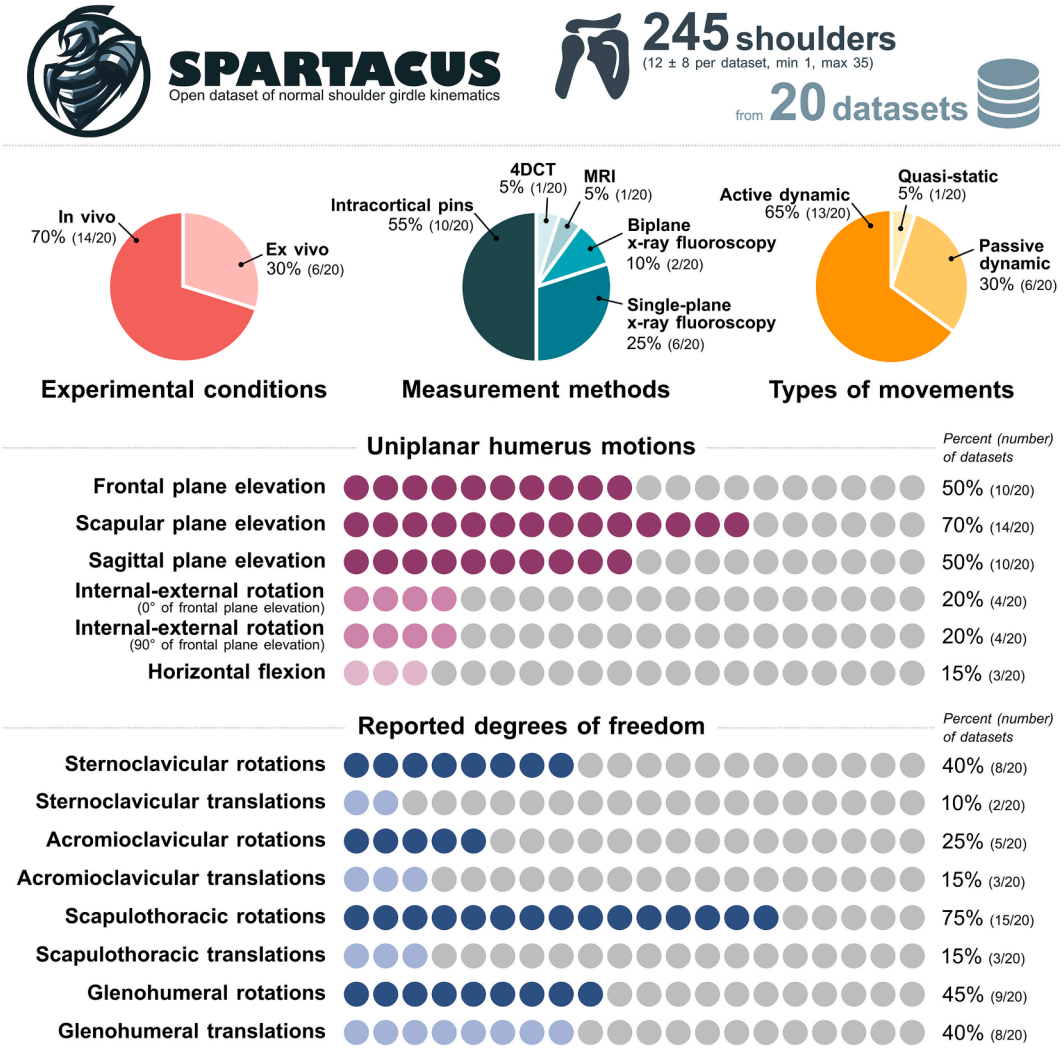

Fig. 1. Composition of the original datasets, including experimental conditions, measurement methods, movement types, uniplanar humerus motions, and reported degrees of freedom. Note: the full list of the 76 extracted features is provided on the GitHub repository (Moissenet et al., 2025).

challenging. To address these discrepancies, we proposed a set of mathematical correction methods using a systematic, well-documented procedure, allowing for more reliable data comparisons. We have combined 20 original datasets into an open-access dataset, named Spartacus, which is available for future research.

4.1. Original datasets

In line with our first aim, we identified 20 original datasets from 30 sources, covering the 24 shoulder girdle DoFs (4 joints × 6 DoFs per joint). These datasets encompass various experimental conditions (i.e., *in vivo*, *ex vivo*), measurement methods (i.e., intracortical pins, 3D imaging), types of movements (i.e., quasi-static, passive dynamic, active dynamic), uniplanar humerus motions (i.e., elevation in several planes, internal-external rotations, horizontal flexion). However, these datasets are too sparse or have insufficient sample sizes to enable a population-wide analysis of normal shoulder girdle kinematics. Aggregating these original datasets has resulted in an open dataset, called Spartacus (Moissenet et al., 2025). This dataset aims at 1) facilitating comparisons between datasets derived from both *ex vivo* and *in vivo* experiments with varying measurement and kinematic processing methods, and 2) enabling a more comprehensive understanding of normal shoulder girdle kinematics.

Most datasets (14 out of 20) in Spartacus were acquired from *in vivo* experimental conditions. While *ex vivo* conditions are valuable for detailed anatomical studies, they are limited to passive motions. In contrast, *in vivo* datasets capture passive and active movements, with preserved muscle activity. This makes them more suitable for meaningful comparisons with common non-invasive measurement methods used across healthy and pathological populations, enhancing their clinical and biomechanical relevance.

About half studies (9 out of 20) in Spartacus are based on imaging technologies although intracortical bone pins, tracked by conventional motion capture systems, have long been considered the gold-standard for kinematic measurements. Recent studies have increasingly relied on imaging techniques. This shift is likely due to both the invasiveness of intracortical bone pins (Hajizadeh et al., 2019) and recent advancements in dynamic imaging technologies (Kwong et al., 2015; Setliff and Anderst, 2024). These advancements reduce reliance on invasive methods and offer greater participant comfort while maintaining high accuracy in capturing joint kinematics. It is expected that the use of imaging-based measurement methods, leading to joint-based LCS (see section 3.2), will continue to grow in the future with the challenge of allowing data comparison with segment-based LCS, recommended by the ISB and often applied when using marker-based or markerless motion capture, and inertial measurement units. Therefore, the extension of the average rotation matrices proposed by Kolz et al. (2020) to the joint-based LCS would allow such comparisons.

Although functional motions more accurately reflect activities of daily living (ADLs), uniplanar humerus motions are generally preferred

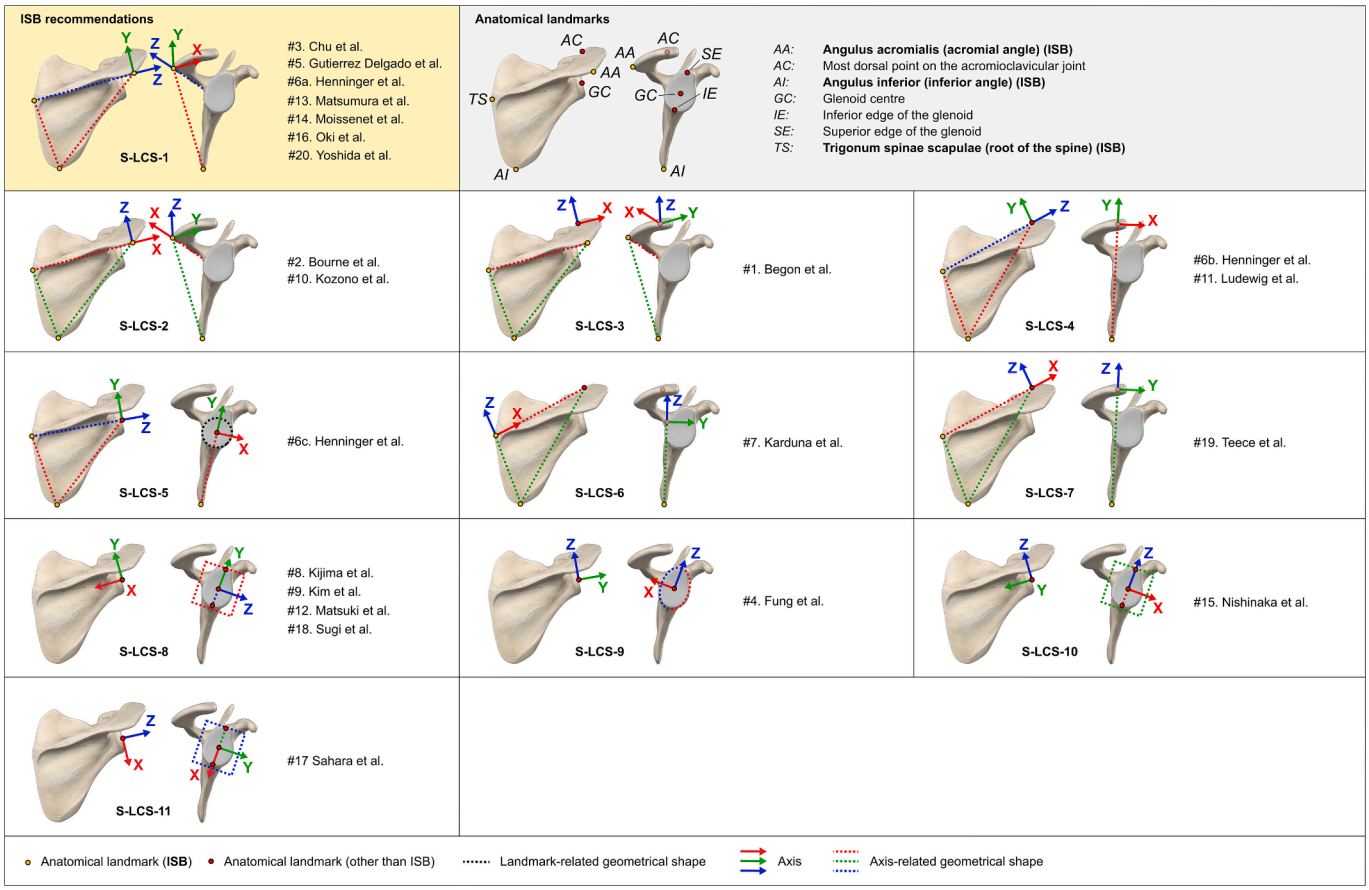

Fig. 2. Variety of scapula local coordinate systems identified across the original datasets (ISB: International Society of Biomechanics). Other tables for the thorax, the clavicle, and the humerus are available in supplementary materials.

in clinical biomechanics because they allow for a clearer description of shoulder rhythm (Krishnan et al., 2019). Motions such as touching the head or reaching for an object were excluded from Spartacus for this reason. Joint kinematics of uniplanar humerus motions are easier to interpret, as most variations occur at a single Euler angle of the thoracohumeral joint, simplifying the analysis of shoulder movement. Elevation movements, particularly scapular plane elevation, were a primary focus in the datasets, likely because of their strong association with shoulder disorders like rotator cuff tears and impingement syndromes (McClure et al., 2006). In the future, records related to ADLs in the included datasets will be reported as additional metadata, further enhancing data availability.

Concerning the reported DoFs, it must be noted that only two datasets (#1, #14) included all DoFs, with 2 shoulders analysed *in vivo* and 10 shoulders *ex vivo*, respectively. Most studies focused on joint rotations, except for the glenohumeral joint, where rotations and translations were examined. Understanding glenohumeral translations in healthy individuals is essential for identifying pathomechanisms such as the ones caused by rotator cuff tears that can alter load distribution and cause superior humeral head translation, compromising glenohumeral stability (Longo et al., 2012). Nevertheless, the literature highlighted the need for detailed kinematic data to assess injuries and the biomechanical impact of treatments on other shoulder joints, such as the acromioclavicular joint (Peeters et al., 2021; Reid et al., 2012). While understanding acromioclavicular joint translations is clinically relevant (Peeters et al., 2021), they were often excluded from kinematic analysis or limited to *ex vivo* studies. Only two datasets (#1, #17) reported reference *in vivo* acromioclavicular joint translations. Overall, acromioclavicular joint assessment is often excluded from *in vivo* analyses. Whereas imaging/ionising techniques (e.g., CT, fluoroscopy) are generally preferred over intracortical bone pins for healthy participants, they are not recommended for the thorax region, particularly because the thyroid gland, located near the clavicle, is highly sensitive to radiation. The availability of more complete gold-standard datasets is critical for clinicians to assess treatment protocols and ultimately improve patient outcomes.

Among the reported DoFs, scapulothoracic rotations were the most extensively studied. Their significant impact on shoulder mobility (e.g., scapulohumeral rhythm (Yano et al., 2010)), stability (Von Eisenhart-Rothe et al., 2005), and their role in injury prevention and rehabilitation (e.g., scapular dyskinesis management (Kibler, 2003)) may explain this focus. Additionally, the traditional difficulty in measuring the scapular motion has contributed to this emphasis, as early studies relied on invasive methods such as intracortical pins (e.g., Dal Maso et al., 2014), while more recent advances in imaging have enabled more accurate assessments without soft tissue artefact (e.g., Kolz et al., 2021). The scapulothoracic joint also presents considerable challenges in biomechanical modeling, with its validation remaining a major hurdle for clinical application (Hu et al., 2020; Naaim et al., 2017; Seth et al., 2016).

4.2. *Compliance with the ISB recommendations*

The ISB recommendations have been a key reference for reporting joint kinematics over the past two decades. In line with our second aim, the present study identified six deviations leading to non-equivalent local coordinate systems and joint kinematics computation methods. These deviations have hindered the comparability of joint kinematics between studies.

Table 2
Deviations from the International Society of Biomechanics (ISB) recommendations (Wu et al., 2005), correction or compensation applied in this study, and recommendations to avoid them.

ID	Deviation	About	Correction or compensation applied	Recommendations to avoid it
D1	1	Orientation of the LCS axes	Corrected by applying a rotation matrix which adjusted the orientation of the distal (or proximal) LCS axes with an intermediate ISB-oriented frame	Clear definition and consistent reporting of the axis labelling conventions in all documents associated with a dataset
D2	2	Method for constructing at least one LCS axis	Compensated using the averaged rotation matrices proposed by Kolz et al. (2020) for the scapula LCS	Sharing of motion capture data and bone surface models to facilitate kinematics re-computations
D3	3	LCS origin	Not corrected nor compensated	Sharing of motion capture data and bone surface models to facilitate kinematics re-computations
D4	4	Euler sequence used to express joint rotations	Corrected by computing joint rotations from the resulting rotation matrix using the Euler sequence recommended by the ISB	Sharing of average quaternions or rotations matrices to express joint rotations in a common coordinate system
D5	5	Coordinate system used to express joint translations	Corrected by adapting previous transformations to express the translation from proximal to distal segment in the proximal LCS	Sharing of average transformation matrices to express joint translations in a common coordinate system
D6	6	Thoracohumeral joint angle computation describing humerus motion	Not corrected nor compensated	Generalising the use of a 3D angle to describe the humerus motion, allowing a common practice across measurement methods, and better reflecting the achieved 3D motion

ISB: International Society of Biomechanics; LCS: Local coordinate system.

4.2.1. Non-equivalent local coordinate systems

Deviations D1 (LCS axis orientation), D2 (LCS axis direction), and D3 (LCS origin) stand for differences in defining the LCS, leading to non-equivalent LCS across studies. Deviations D1 and D2 affect the computation of the 6-DoF kinematics of each shoulder joint, whereas deviation D3 only impacts joint translations. All these deviations were observed in most original datasets. But beyond the compliance with the ISB recommendations, the original datasets exhibited a considerable variety of LCS for each bony segment (8 for the thorax, clavicle, and humerus, 11 for the scapula). Such discrepancies are highly detrimental to the research community, making data comparison extremely challenging or even impossible. Several factors that may have led to these deviations are discussed below, along with recommendations to facilitate data comparison.

Concerning the deviation D1 (LCS axis orientation), one factor can be attributed to the former conventions “y-up” and “z-up” which define the inferosuperior axis (pointing superiorly). The “y-up” convention has been promoted by the ISB recommendations (Cereatti et al., 2024; Wu et al., 2005, 2002), while the “z-up” convention has been promoted notably by the Conventional Gait Model (also known as the Plug-in Gait model) (Leboeuf et al., 2019), another widely used reference for reporting joint kinematics of lower limbs. When the ISB recommendations cannot be strictly applied, the impact of deviation D1 on data comparison can be corrected or minimised by clearly defining and consistently reporting the axis labelling conventions in all documents associated with a dataset (Kontaxis et al., 2009).

Concerning the deviations D2 (LCS axis direction) and D3 (LCS origin), a first factor can be attributed to the selection of anatomical landmarks used to construct each LCS. The variations outlined below are primarily driven by the need to simplify measurements or calculations. For the thorax, the spinous process landmarks were either selected as T1 (please refer to Supplementary material 3 for bony landmark definitions) instead of C7 (#1, #7), or T7/T10 instead of T8 (#1, #2, #3, #7). These decisions are influenced by several thorax models proposed in the literature, leading to known kinematic discrepancies (Armand et al., 2014; Leardini et al., 2009). Additionally, some datasets (#2, #7) excluded the xiphoid process (PX). This choice is often made due to discomfort during palpation, particularly in female participants (Pain et al., 2019), and because of occlusions caused by bras (Ulman et al., 2024). For the clavicle, the definition proposed by the ISB recommendations for the anteroposterior axis, perpendicular to both the clavicle mediolateral axis and the thorax inferosuperior axis, was often modified (see Supplementary material 3) when invasive or ionising methods allowed for direct measurements (#4, #5, #12). For the scapula, the acromial angle (AA) was replaced in several datasets (#1, #2, #3, #5, #6, #7, #10, #11, #13, #14, #16, #19, #20) by the most dorsal point on the acromioclavicular joint (AC) or the glenoid centre (GC), as already pointed out by some recent comparison studies (Kolz et al., 2020; Lawrence et al., 2022; Ludewig et al., 2010). While AC was initially proposed by van der Helm (Van der Helm, 1997), it was replaced by AA in the ISB recommendations to prevent gimbal lock (Wu et al., 2005). In contrast, GC provides better alignment with the centre of the humeral head (De Wilde et al., 2010; Ohl et al., 2015) and results in a better agreement with the instantaneous helical axis, without experiencing gimbal lock (Lawrence et al., 2022). This highlights the advantages of imaging-based measurement methods for accurately locating non-palpable landmarks. It must be noted here that selecting GC over AA can result in differences in ST joint rotations of up to 23° (Kolz et al., 2020). When strict application of ISB recommendations is not feasible, the impact of these deviations on data comparison can be corrected by including additional virtual landmarks in the dataset. These landmarks can be recorded during a calibration trial (Trinler and Baker, 2018), via stylus digitisation (Ludewig et al., 2009), or using imaging measurements (Morrissey et al., 2008), creating a shared minimal set of landmarks across studies to enable consistent re-computation of joint kinematics. In cases where such landmarks are unavailable, a compensation approach using averaged rotation matrices, such as those proposed by Kolz et al. (2020), can facilitate conversion between different LCS. This method could also be extended using statistical shape models to account for inter-subject variability (Huang et al., 2022).

Still concerning the deviations D2 (LCS axis direction) and D3 (LCS origin), a second factor can be attributed to the construction of each LCS using geometric features, such as cylinders or planes, instead of anatomical landmarks. Such an approach allows for more consistent anatomical axis construction that can possibly be semi-automatised (Vlachopoulos et al., 2016). However, it is restricted to the use of

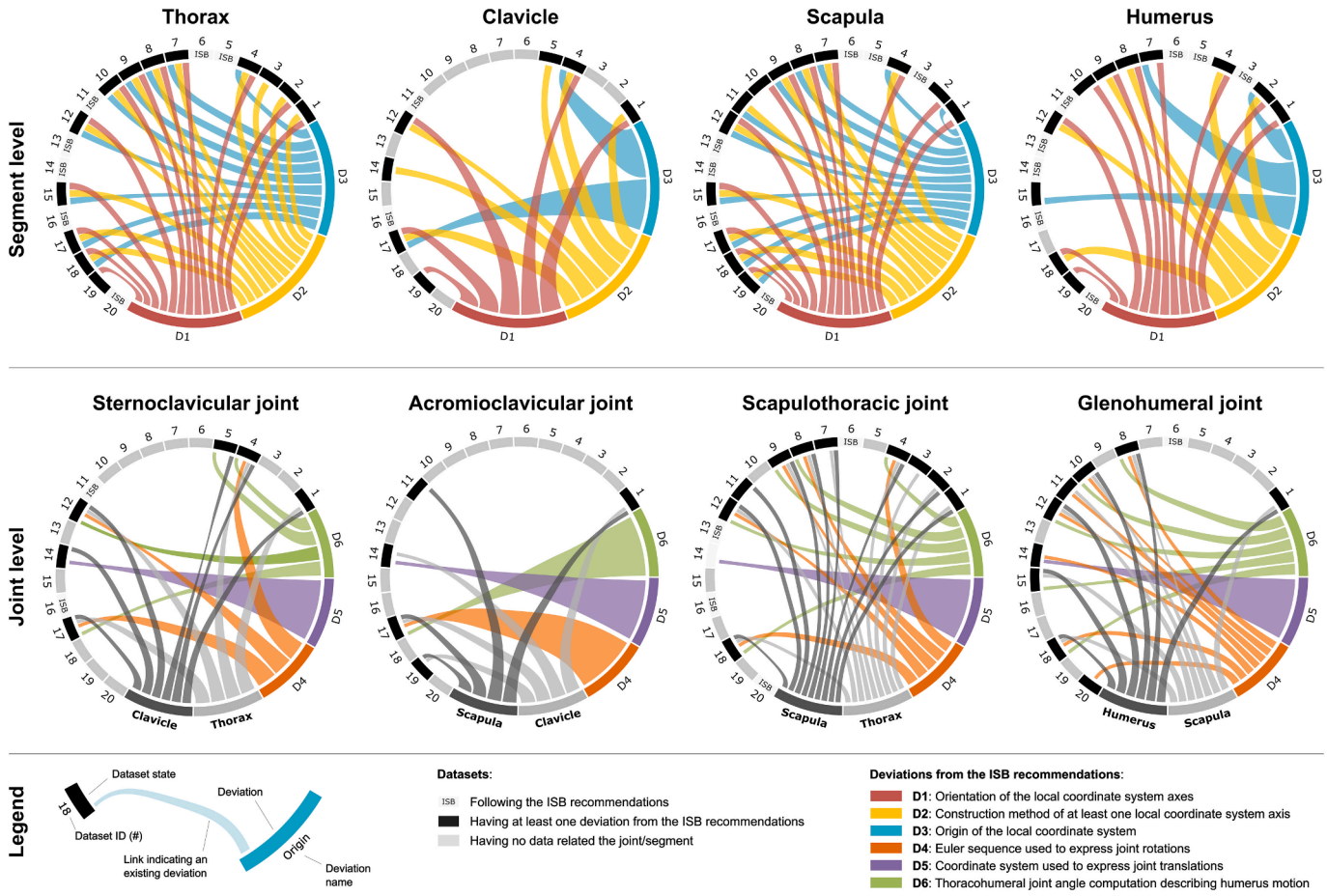

Fig. 3. Deviations from the International Society of Biomechanics (ISB) recommendations (Wu et al., 2005) identified for each original dataset at both segment and joint levels.

imaging-based measurement methods. For the thorax, clavicle, and humerus, best-fit cylinders suited to the spinal canal (#4), the distal part of the clavicle (#17), and the humerus diaphysis (#8, #9, #12, #18) were used to define the thorax inferosuperior axis, the clavicle mediolateral axis, and the humerus inferosuperior axis, respectively. For the scapula, a best-fit plane (#8, #9, #12, #15, #17) and a best-fit ellipse (#4), suited to the glenoid contour, were used to define a glenoid-based coordinate system. Indeed, glenoid-based coordinate systems provide a more precise and clinically relevant reference for describing joint kinematics, especially GH joint translations, than the ISB scapula-based LCS. Although there appears to be a consensus in utilising the major and minor glenoid axes, their definition varies among studies. For the humerus, geometrical methods involving the neck-shaft plane (#18) or the intertubercular groove (#8, #9, #12) were also employed when epicondyles could not be localized. For example, imaging approaches may have a restricted field of view or use a limited scanning area to minimize participant ionization, leading to further inconsistencies in defining LCS axes (#8, #9, #12, #18). Furthermore, in ex vivo experiments, the humerus is sometimes transected to facilitate manipulation by a serial robot (#14). When strict application of ISB recommendations is not feasible, the impact of these deviations on data comparison can be minimised by sharing motion capture data and bone surface models (as observed in #6 and #14), which facilitates kinematics re-computations.

Despite the advantages of imaging methods, all reported imaging-based datasets (#8, #9, #10, #12, #15, #17, #18) except one (#20) skipped defining a thorax LCS, instead expressing sternoclavicular and scapulothoracic joint kinematics based on the imaging system's reference. This highlights a significant limitation of imaging-based measurement methods, due to a restricted field of view, potentially affecting the comprehensiveness of joint kinematic analyses. In this case, the ISB recommendations cannot be applied to the sternoclavicular, scapulothoracic, and thoracohumeral joints, leading to irreparable offsets. However, the impact of these deviations on data comparison can be minimised by combining multiple measurement methods, when possible, to establish a thorax LCS definition (Kolz et al., 2021).

4.2.2. *Non-equivalent joint kinematics computation methods*

Deviations D4 (Euler sequence), D5 (translation coordinate system), and D6 (TH joint angle) stand for calculation differences, leading to non-equivalent joint kinematics computation methods across studies. Deviations D4 and D5 specifically affect joint rotations and translations, respectively, but deviation D6 introduces biases in comparing data across the 6 DoFs. While deviations D4 and D6 were observed in several original datasets, deviation D5 was only observed in one original dataset (#14). These three deviations are mainly led by modelling choices that can imply numerical issues.

The selection of Euler sequences has been frequently debated in the literature (Phadke et al., 2011; Šenk and Chèze, 2006) and is one factor leading to deviation D4 (Euler sequence). In the present study, the deviation D4 was observed in all joints, but most frequently for the glenohumeral joint (#8, #10, #11, #12, #14, #18, #20). Indeed, the ISB-recommended YX'Y'' sequence (Y representing the plane of elevation, 0° for abduction and 90° for flexion, X' the elevation angle (negative), and Y'' the humeral axial rotation) has faced criticism due to its susceptibility to gimbal lock (Phadke et al., 2011; Šenk and Chèze, 2006). Moreover, extracting angles based on a YX'Y'' sequence often produces values outside physiological ranges, due to issues with non-uniqueness and standard matrix identification methods that fail to yield

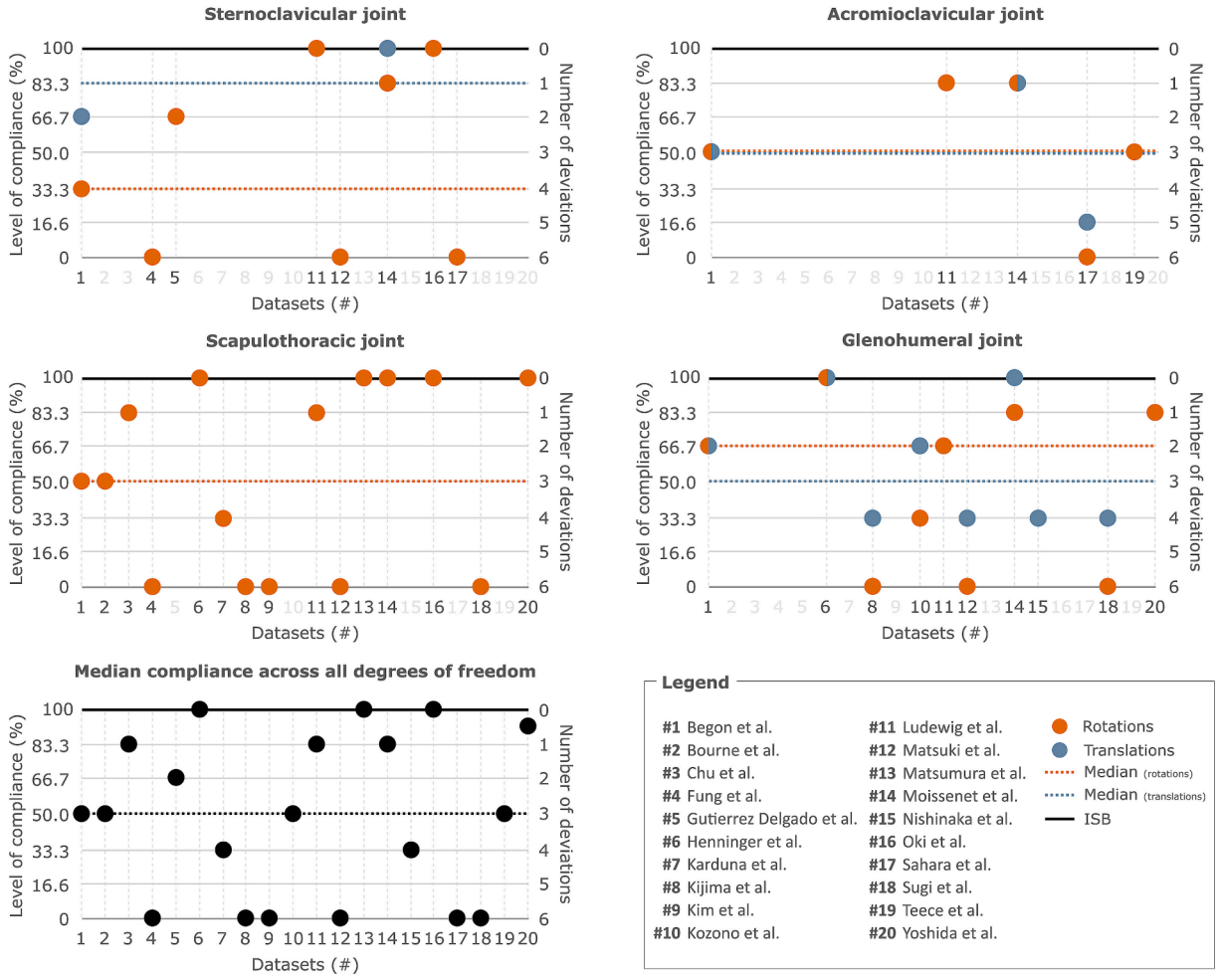

Fig. 4. Compliance scores with the International Society of Biomechanics (ISB) recommendations (Wu et al., 2005) obtained for each original dataset (and the median value), for each joint, and for both rotations and displacements, in percentage (100%, of the 6 related deviations, corresponds to a dataset applying strictly the ISB recommendations, i.e., no deviation. An empty column means that the degree of freedom was not considered in the dataset. Scapulothoracic translations are not defined in the ISB recommendations). The median compliance score across all degrees of freedom is also reported.

interpretable results (see the work of Aliaj et al. (2021) for a reliable alternative). Hence, there is no universally ideal sequence for describing glenohumeral joint rotations across all ranges and planes. For instance, alternative sequences like YX'Z'', ZX'Y'', and XZ'Y'' (according to the ISB axis definition) are more suitable for specific movements (Šenk and Chèze, 2006). While the choice of Euler sequences may be justified by experimental conditions (and is probably the most reasonable reason not to use the ISB recommendations), it complicates comparisons of joint rotations across studies, particularly affecting computed angular amplitudes (Karduna et al., 2000). When the ISB recommendations are respected, the impact of this deviation on data comparison can be corrected or minimised by encouraging data sharing, such as quaternions or rotation matrices, to re-compute joint rotations with the ISB-recommended Euler sequence (or any other Euler sequence).

Two approaches for expressing the joint translations have been promoted by the ISB recommendations, depending on the joint of interest (Wu et al., 2005) and may partly explain deviation D5 (translation coordinate system). On one hand, for the radioulnar, interphalangeal, metacarpophalangeal, intercarpal, radiocarpal, and carpometacarpal joints (as well as for the lower limb and spine joints (Wu et al., 2002)), the joint coordinate system (JCS) is recommended to express the joint translations. While allowing to express joint translations along the axes used to report joint rotations, this approach requires a method to express any 3D vector in a non-orthogonal coordinate system (such as the JCS) (Desroches et al., 2010; Dumas et al., 2012). On the other hand, for the scapulothoracic, acromioclavicular, and glenohumeral joints, the proximal LCS is recommended to express the joint translations. It must be noted that no recommendation was made for the scapulothoracic and thoracohumeral joints. All reported datasets except one (#14) used the proximal LCS to express the joint translations. In the dataset #14, the approach proposed by Desroches et al. (2010) was used to achieve a non-orthogonal coordinate system projection and applied to all joints of the shoulder girdle, including the scapulothoracic joint. When the ISB recommendations are not respected, the impact of this deviation on data comparison can be corrected or minimised by encouraging data sharing, such as homogeneous matrices, to re-compute joint translations with the ISB-recommended coordinate system (or any other coordinate system).

The measurement and calculation of the thoracohumeral joint angle varies in practice and lead to the deviation D6 (thoracohumeral angle). In imaging-based datasets lacking a thorax LCS, researchers have fallen back on computing the 3D angle between the longitudinal humeral axis and the imaging system's vertical axis (#5, #8, #9, #12, #15, #18) or determining arm angle with goniometers (#17). Moreover, the chosen Euler angle was not mentioned in all of the 13 datasets using an YX'Y'' sequence or equivalent (#1, #2, #3, #4, #6, #7, #10, #11, #13, #14, #16, #19, #20) and was thus guessed during the processing. In the case of elevation movements, we expect to express the main thoracohumeral motion around X', whereas Y'' is chosen for analysing internal-external rotation movements. It is also accepted to display and analyse joint

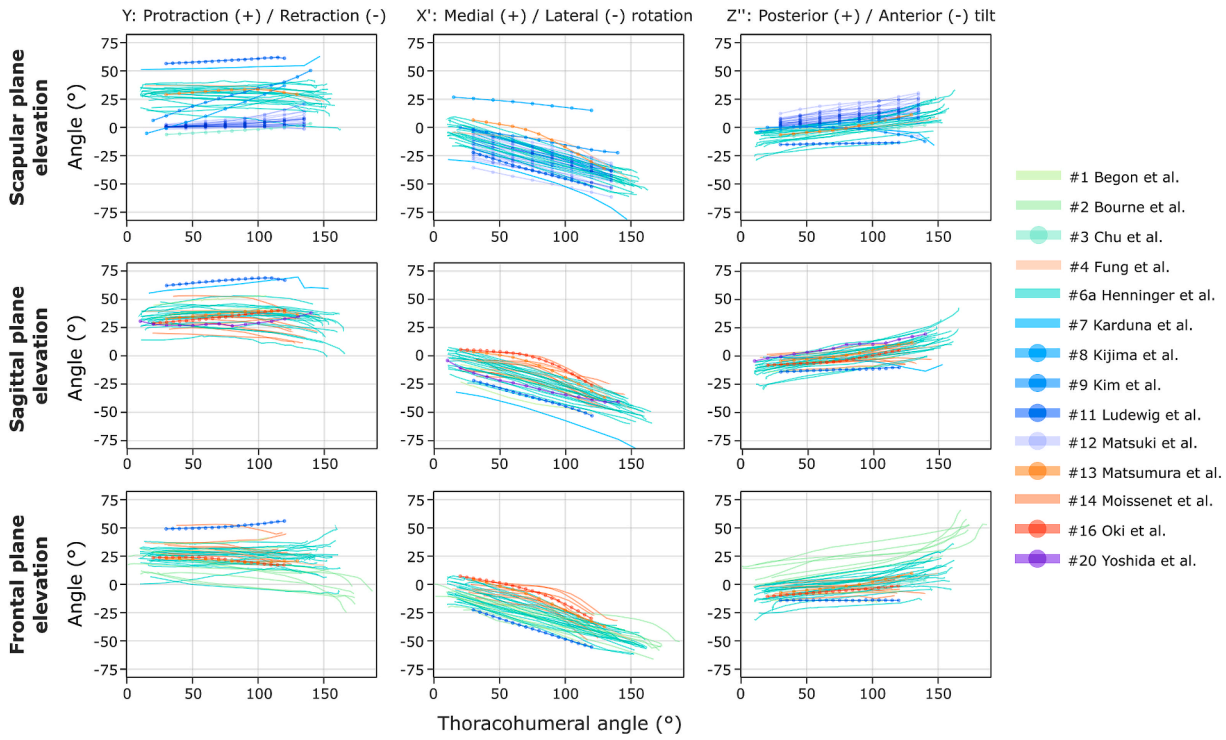

Fig. 5. Frontal, sagittal, and scapular plane elevation angles from consolidated datasets following the International Society of Biomechanics recommendations (Wu et al., 2005). Ex vivo measurements are shown in warm colors.

angles or translations as a function of a single thoracohumeral joint angle as this chosen angle best represents the global humerus motion. This approach is clinically relevant and appropriate for interpretations of the analytical motions reported in Spartacus but is insufficient for more complex motions. No ISB recommendation currently exists for this practice. Analyses based on a single thoracohumeral angle should be defined by systematically measuring it in 3D, specifying the Euler sequence used for calculation, and clearly reporting the chosen angle. Additionally, sharing the global orientation of the humerus would help to correct or compensate deviations and provide a more accurate 3D motion, paving the way for future studies.

To summarise, this study highlighted significant discrepancies among original datasets and limited compliance with the ISB recommendations, making direct comparisons particularly challenging. A key strength of Spartacus is the mathematical correction of these deviations using a systematic, well-documented procedure, enabling more reliable data comparisons, and discussed hereafter.

4.3. *Unified convention for kinematics re-processing*

Significant efforts were dedicated to unifying datasets by gathering the information needed for kinematic re-processing, to merge data and compare them. However, only deviations D1 (LCS axis orientation), D4 (Euler sequence), and D5 (translation coordinate system) could be systematically corrected. Other deviations were only at best compensated, leaving the appreciation to the user of Spartacus to evaluate if it is enough to be considered as confident data. A compliance score was provided for each dataset to help the user in this choice. This issue could be avoided by promoting good practices in open science. Indeed, most authors only share data as kinematic series reported as curves and representing the mean values across participants. For Spartacus, these curves were manually digitised in 10 out of 20 datasets. Unfortunately, Euler angles are not independent of each other and treating them as vectors (e.g., subtraction or mean) leads to mathematically flawed and incorrect interpretations (Michaud et al., 2014; Woltring, 1991), especially after the corrections required to respect the ISB recommendations. Sharing average quaternions for means or Euler angles for each participant would better maintain the accuracy and integrity of kinematic data. In line with open science, providing full access to raw datasets, analysis code, and detailed methodologies (e.g., datasets #6 and #14) ensures reproducibility, fosters collaboration, and accelerates progress across the field.

Correction methods for the deviations D2 (LCS axis direction) and D3 (LCS origin) would necessitate for each participant either 1) extra anatomical landmark coordinates or 2) raw motion capture data together with bone surface models to re-identify these landmarks or geometrical features. Unfortunately, only two original datasets (#6, #14) included bone surface models, and none provided additional anatomical landmarks beyond those used to define original LCS. As a result, deviation D3 could not be corrected nor compensated, and deviation D2 was compensated, when possible, using the method proposed by Kolz et al. (2020). While simple and demonstrating good accuracy ($4.0 \pm 3.0°$ error in scapulothoracic kinematics (Kolz et al., 2020)), this approach falls short of true correction. This is because it relies on rotation matrices averaged across a population, whereas providing additional anatomical landmarks would allow for the true calculation of ISB-oriented LCS and kinematics. Extending this method to other LCS, particularly glenoid-based systems and other bones, could be valuable. Notably, the same approach has already been applied to the humerus LCS by Sulkar et al. (2021), though the proposed rotation matrices did not apply to the present datasets.

To introduce population-based variability, statistical shape models could be used to generate a set of bone surface models, annotated with anatomical landmarks, to compute average rotation matrices allowing the transformation from a LCS to another one. Although this approach would be more challenging for the clavicle due to its high shape variability (Bernat et al., 2014), it could significantly benefit the thorax regarding the multiple spinal processes used to define its LCS.

Overall, this study lays the foundation for a broader consideration on best practices in data sharing and correction/compensation methods for kinematics re-processing. The systematic, well-documented procedure facilitates the comparison and merging of data and could be adapted to other joints.

4.4. Limitations

This study has several limitations. First, we did not conduct a systematic review. Some datasets might thus be omitted. Furthermore, some additional datasets have been published by the time this paper was reviewed, such as a more complete dataset proposed by Henninger (2024). However, a framework is now available within Spartacus and the community is welcome to contribute. Second, each deviation might not have the same impact on joint kinematics. However, current datasets do not allow for establishing hierarchy or metric. The impact of each deviation could be quantified using a unique dataset allowing to compute joint kinematics using all observed variations in LCS definition and in joint kinematics computation. Furthermore, we observed that the kinematic consequences of these deviations produced errors of similar magnitudes to the inter-participant variability, making it more challenging to identify individual contributions and reinforcing the need to avoid such deviations. Third, the present study only focused on datasets related to gold-standard measurement methods. Thus, it does not necessarily reflect deviations in overall practice when non-invasive and non-ionising measurement methods are used. Techniques such as optical marker tracking, inertial measurement units, or markerless motion tracking constitute a significantly larger portion of the literature on shoulder kinematics. It would thus be interesting to perform a larger review to observe how much the ISB recommendations are applied and if a revised version would be required to better fill the current needs of the community.

4.5. Conclusion

This study provides an aggregation of 20 original datasets consisting of recordings from 245 shoulders measured using 5 different measurement methods and during 6 different uniplanar humerus motions. The aggregated data will 1) enable a more comprehensive understanding of normal shoulder girdle kinematics and 2) facilitate comparisons between datasets derived from both *ex vivo* and *in vivo* experiments with varying measurement and kinematic processing methods. More importantly, the authors claim the need for more conventional reporting, through a unified checklist (an example is provided in Supplementary material 4), the generalisation of homogeneous matrix sharing, and perhaps the need for a revision of the current ISB recommendations. Such a revision should establish a clear framework enabling the data comparison across multiple measurement methods and experimental conditions, as well as the reprocessing of data.

CRediT authorship contribution statement

Florent Moissenet: Writing – review & editing, Writing – original draft, Visualization, Validation, Supervision, Resources, Methodology, Investigation, Formal analysis, Data curation, Conceptualization. **Pierre Puchaud:** Writing – review & editing, Visualization, Validation, Software, Resources, Methodology, Investigation, Formal analysis, Data curation. **Alexandre Naaim:** Writing – review & editing, Validation, Software, Methodology, Investigation, Formal analysis, Data curation. **Nicolas Holzer:** Writing – review & editing, Project administration, Funding acquisition. **Mickaël Begon:** Writing – review & editing, Writing – original draft, Resources, Project administration, Funding acquisition.

Declaration of competing interest

The authors declare that they have no known competing financial interests or personal relationships that could have appeared to influence the work reported in this paper.

Acknowledgments

The authors are very grateful to the teams who made their datasets available. This adds considerable value to our work. This project was made possible thanks to the LIA-EVASYM shared laboratory.

Appendix A

To handle data collected from left shoulders, an additional correction was applied by converting the rotation matrix ${}^{P}\mathbf{R}_{D}$ from the left side to the right side. This adjustment ensures consistency when comparing datasets as if they were collected from right shoulders. This process is equivalent to converting to a left-handed rotation matrix by applying the following transformation:

$$ {}^{P}\mathbf{R}_{D}^{right} = diag(1,1,-1)\cdot {}^{P}\mathbf{R}_{D}^{left}\cdot \mathrm{diag}(1,1,-1)^{\mathrm{T}} \tag{3} $$

where $\mathrm{diag}(k)$ represents a diagonal matrix where all diagonal elements are k, and all off-diagonal elements are zero.

Appendix B. Supplementary data

Supplementary data to this article can be found online at https://doi.org/10.1016/j.jbiomech.2025.112642.

Data availability

The reader can find the following five documents as supplementary materials:

(SM1) a summary of the ISB recommendations

(SM2) an explanatory note on the compliance metric

(SM3) definition of all LCS found in this review

(SM4) a checklist for experimenters to ensure a proper kinematic reprocessing of their shoulder kinematic data

(SM5) the demographic data from the included studies

The Spartacus dataset and the code used to correct or compensate for the observed deviations are open-sourced and freely available on the following GitHub repository: https://github.com/Spartacus-shoulder-kinematics-dataset/shoulder-kinematics.

References

Aliaj, K., Foreman, K.B., Chalmers, P.N., Henninger, H.B., 2021. Beyond Euler/Cardan analysis: True glenohumeral axial rotation during arm elevation and rotation. Gait. Posture 88, 28–36. https://doi.org/10.1016/j.gaitpost.2021.05.004.

Aliaj, K., Lawrence, R.L., Bo Foreman, K., Chalmers, P.N., Henninger, H.B., 2022. Kinematic coupling of the glenohumeral and scapulothoracic joints generates

humeral axial rotation. J. Biomech. 136, 111059. https://doi.org/10.1016/j.jbiomech.2022.111059.
Armand, S., Sangeux, M., Baker, R., 2014. Optimal markers' placement on the thorax for clinical gait analysis. Gait. Posture 39, 147–153. https://doi.org/10.1016/j.gaitpost.2013.06.016.
Bernat, A., Huysmans, T., Van Glabbeek, F., Sijbers, J., Gielen, J., Van Tongel, A., 2014. The anatomy of the clavicle: A Three-dimensional Cadaveric Study. Clin. Anat. 27, 712–723. https://doi.org/10.1002/ca.22288.
Blache, Y., Begon, M., 2018. Influence of Shoulder Kinematic Estimate on Joint and Muscle Mechanics Predicted by Musculoskeletal Model. IEEE. Trans. Biomed. Eng. 65, 715–722. https://doi.org/10.1109/TBME.2017.2716186.
Blache, Y., Dumas, R., Lundberg, A., Begon, M., 2017. Main component of soft tissue artifact of the upper-limbs with respect to different functional, daily life and sports movements. J. Biomech. 62, 39–46. https://doi.org/10.1016/j.jbiomech.2016.10.019.
Bourne, D.A., 2009. Accuracy and reliability of a new method of measuring three-dimensional scapular kinematics. Doi: 10.14288/1.0091259.
Bourne, D.A., Choo, A.M.T., Regan, W.D., MacIntyre, D.L., Oxland, T.R., 2007. Three-dimensional rotation of the scapula during functional movements: An in vivo study in healthy volunteers. J. Shoulder. Elbow. Surg. 16, 150–162. https://doi.org/10.1016/j.jse.2006.06.011.
Cereatti, A., Bonci, T., Akbarshahi, M., Aminian, K., Barré, A., Begon, M., Benoit, D.L., Charbonnier, C., Dal Maso, F., Fantozzi, S., Lin, C.-C., Lu, T.-W., Pandy, M.G., Stagni, R., Van Den Bogert, A.J., Camomilla, V., 2017. Standardization proposal of soft tissue artefact description for data sharing in human motion measurements. J. Biomech. 62, 5–13. https://doi.org/10.1016/j.jbiomech.2017.02.004.
Cereatti, A., Gurchiek, R., Mündermann, A., Fantozzi, S., Horak, F., Delp, S., Aminian, K., 2024. ISB recommendations on the definition, estimation, and reporting of joint kinematics in human motion analysis applications using wearable inertial measurement technology. J. Biomech. 173, 112225. https://doi.org/10.1016/j.jbiomech.2024.112225.
Chu, Y., Akins, J., Lovalekar, M., Tashman, S., Lephart, S., Sell, T., 2012. Validation of a video-based motion analysis technique in 3-D dynamic scapular kinematic measurements. J. Biomech. 45, 2462–2466. https://doi.org/10.1016/j.jbiomech.2012.06.025.
Como, C., LeVasseur, C., Kane, G., Rai, A., Munsch, M., Gabrielli, A., Hughes, J., Anderst, W., Lin, A., 2022. Implant characteristics affect in vivo shoulder kinematics during multiplanar functional motions after reverse shoulder arthroplasty. J. Biomech. 135, 111050. https://doi.org/10.1016/j.jbiomech.2022.111050.
Cools, A.M., Maenhout, A.G., Vanderstukken, F., Declève, P., Johansson, F.R., Borms, D., 2021. The challenge of the sporting shoulder: From injury prevention through sport-specific rehabilitation toward return to play. Ann. Phys. Rehabil. Med. 64, 101384. https://doi.org/10.1016/j.rehab.2020.03.009.
Dal Maso, F., Raison, M., Lundberg, A., Arndt, A., Begon, M., 2014. Coupling between 3D displacements and rotations at the glenohumeral joint during dynamic tasks in healthy participants. Clin. Biomech. 29, 1048–1055. https://doi.org/10.1016/j.clinbiomech.2014.08.006.
De Wilde, L.F., Verstraeten, T., Speeckaert, W., Karelse, A., 2010. Reliability of the glenoid plane. J. Shoulder. Elbow. Surg. 19, 414–422. https://doi.org/10.1016/j.jse.2009.10.005.
Desroches, G., Chèze, L., Dumas, R., 2010. Expression of Joint Moment in the Joint Coordinate System. J. Biomech. Eng. 132, 114503. https://doi.org/10.1115/1.4002537.
Dumas, R., Robert, T., Pomero, V., Cheze, L., 2012. Joint and segment coordinate systems revisited. Comput. Methods. Biomech. Biomed. Eng. 15, 183–185. https://doi.org/10.1080/10255842.2012.713646.
Duprey, S., Naaim, A., Moissenet, F., Begon, M., Chèze, L., 2017. Kinematic models of the upper limb joints for multibody kinematics optimisation: An overview. J. Biomech. 62, 87–94. https://doi.org/10.1016/j.jbiomech.2016.12.005.
Fung, M., Kato, S., Barrance, P.J., Elias, J.J., McFarland, E.G., Nobuhara, K., Chao, E.Y., 2001. Scapular and clavicular kinematics during humeral elevation: A study with cadavers. J. Shoulder. Elbow. Surg. 10, 278–285. https://doi.org/10.1067/mse.2001.114496.
Gasparutto, X., Moissenet, F., Lafon, Y., Chèze, L., Dumas, R., 2017. Kinematics of the Normal Knee during Dynamic Activities: A Synthesis of Data from Intracortical Pins and Biplane Imaging. Appl. Bionics. Biomech. 2017, 1–9. https://doi.org/10.1155/2017/1908618.
Gutierrez Delgado, G., De Beule, M., Ortega Cardentey, D.R., Segers, P., Iznaga Benítez, A.M., Rodríguez Moliner, T., Verhegghe, B., Palmans, T., Van Hoof, T., Van Tongel, A., 2017. Procedure to describe clavicular motion. J. Shoulder. Elbow. Surg. 26, 490–496. https://doi.org/10.1016/j.jse.2016.09.009.
Haering, D., Raison, M., Begon, M., 2014. Measurement and Description of Three-Dimensional Shoulder Range of Motion With Degrees of Freedom Interactions. J. Biomech. Eng. 136, 084502. https://doi.org/10.1115/1.4027665.
Hajizadeh, M., Michaud, B., Begon, M., 2019. The effect of intracortical bone pin on shoulder kinematics during dynamic activities. Int. Biomech. 6, 47–53. https://doi.org/10.1080/23335432.2019.1633958.
Henninger, H.B., 2024. Shoulder kinematics derived from radiographic and optical motion analysis (Version v1). Dataset,. Zenodo. https://doi.org/10.5281/zenodo.10972005.
Hu, T., Kühn, J., Haddadin, S., 2020. Forward and inverse dynamics modeling of human shoulder-arm musculoskeletal system with scapulothoracic constraint. Comput. Methods. Biomech. Biomed. Eng. 23, 785–803. https://doi.org/10.1080/10255842.2020.1764945.
Huang, Y., Robinson, D.L., Pitocchi, J., Lee, P.V.S., Ackland, D.C., 2022. Glenohumeral joint reconstruction using statistical shape modeling. Biomech. Model. Mechanobiol. 21, 249–259. https://doi.org/10.1007/s10237-021-01533-6.
Karduna, A.R., McClure, P.W., Michener, L.A., 2000. Scapular kinematics: effects of altering the Euler angle sequence of rotations. J. Biomech. 33, 1063–1068. https://doi.org/10.1016/S0021-9290(00)00078-6.
Kibler, B.W., 2003. Management of the Scapula in Glenohumeral Instability. Tech. Should. Elbow. Surg. 4, 89–98. https://doi.org/10.1097/00132589-200309000-00001.
Kijima, T., Matsuki, K., Ochiai, N., Yamaguchi, T., Sasaki, Yu., Hashimoto, E., Sasaki, Y., Yamazaki, H., Kenmoku, T., Yamaguchi, S., Masuda, Y., Umekita, H., Banks, S.A., Takahashi, K., 2015. In vivo 3-dimensional analysis of scapular and glenohumeral kinematics: comparison of symptomatic or asymptomatic shoulders with rotator cuff tears and healthy shoulders. J. Shoulder. Elbow. Surg. 24, 1817–1826. https://doi.org/10.1016/j.jse.2015.06.003.
Kim, D., Lee, D., Jang, Y., Yeom, J., Banks, S.A., 2017. Effects of short malunion of the clavicle on in vivo scapular kinematics. J. Shoulder. Elbow. Surg. 26, e286–e292. https://doi.org/10.1016/j.jse.2017.03.013.
Kolz, C.W., Sulkar, H.J., Aliaj, K., Tashjian, R.Z., Chalmers, P.N., Qiu, Y., Zhang, Y., Bo Foreman, K., Anderson, A.E., Henninger, H.B., 2021. Age-related differences in humerothoracic, scapulothoracic, and glenohumeral kinematics during elevation and rotation motions. J. Biomech. 117, 110266. https://doi.org/10.1016/j.jbiomech.2021.110266.
Kolz, C.W., Sulkar, H.J., Aliaj, K., Tashjian, R.Z., Chalmers, P.N., Qiu, Y., Zhang, Y., Foreman, K.B., Anderson, A.E., Henninger, H.B., 2020. Reliable interpretation of scapular kinematics depends on coordinate system definition. Gait. Posture 81, 183–190. https://doi.org/10.1016/j.gaitpost.2020.07.020.
Kontaxis, A., Cutti, A.G., Johnson, G.R., Veeger, H.E.J., 2009. A framework for the definition of standardized protocols for measuring upper-extremity kinematics. Clin. Biomech. 24, 246–253. https://doi.org/10.1016/j.clinbiomech.2008.12.009.
Kozono, N., Okada, T., Takeuchi, N., Hamai, S., Higaki, H., Ikebe, S., Shimoto, T., Miake, G., Nakanishi, Y., Iwamoto, Y., 2017. In vivo kinematic analysis of the glenohumeral joint during dynamic full axial rotation and scapular plane full abduction in healthy shoulders. Knee. Surg. Sports. Traumatol. Arthrosc 25, 2032–2040. https://doi.org/10.1007/s00167-016-4263-2.
Krishnan, R., Björsell, N., Gutierrez-Farewik, E.M., Smith, C., 2019. A survey of human shoulder functional kinematic representations. Med. Biol. Eng. Comput. 57, 339–367. https://doi.org/10.1007/s11517-018-1903-3.
Krzywinski, M., Schein, J., Birol, İ., Connors, J., Gascoyne, R., Horsman, D., Jones, S.J., Marra, M.A., 2009. Circos: An information aesthetic for comparative genomics. Genome. Res. 19, 1639–1645. https://doi.org/10.1101/gr.092759.109.
Kwong, Y., Mel, A.O., Wheeler, G., Troupis, J.M., 2015. F our-dimensional computed tomography (4DCT): A review of the current status and applications. J. Med. Imag. Rad. Onc 59, 545–554. https://doi.org/10.1111/1754-9485.12326.
Lawrence, R.L., Braman, J.P., Staker, J.L., Laprade, R.F., Ludewig, P.M., 2014. Comparison of 3-dimensional shoulder complex kinematics in individuals with and without shoulder pain, part 2: glenohumeral joint. J. Orthop. Sports. Phys. Ther 44 (646–655), B1–B3. https://doi.org/10.2519/jospt.2014.5556.
Lawrence, R.L., Roseni, K., Bey, M.J., 2022. Correspondence between scapular anatomical coordinate systems and the 3D axis of motion: A new perspective on an old challenge. J. Biomech. 145, 111385. https://doi.org/10.1016/j.jbiomech.2022.111385.
Leardini, A., Biagi, F., Belvedere, C., Benedetti, M.G., 2009. Quantitative comparison of current models for trunk motion in human movement analysis. Clin. Biomech. 24, 542–550. https://doi.org/10.1016/j.clinbiomech.2009.05.005.
Leboeuf, F., Baker, R., Barré, A., Reay, J., Jones, R., Sangeux, M., 2019. The conventional gait model, an open-source implementation that reproduces the past but prepares for the future. Gait. Posture 69, 235–241. https://doi.org/10.1016/j.gaitpost.2019.04.015.
Longo, U.G., Berton, A., Papapietro, N., Maffulli, Nicola, Denaro, V., 2012. Biomechanics of the Rotator Cuff: European Perspective, in: Maffulli, N. (Ed.), Medicine and Sport Science. S. Karger AG, pp. 10–17. Doi: 10.1159/000328870.
Longo, U.G., De Salvatore, S., Carnevale, A., Tecce, S.M., Bandini, B., Lalli, A., Schena, E., Denaro, V., 2022. Optical motion capture systems for 3D kinematic analysis in patients with shoulder disorders. IJERPH 19, 12033. https://doi.org/10.3390/ijerph191912033.
Ludewig, P.M., Hassett, D.R., LaPrade, R.F., Camargo, P.R., Braman, J.P., 2010. Comparison of scapular local coordinate systems. Clin. Biomech. 25, 415–421. https://doi.org/10.1016/j.clinbiomech.2010.01.015.
Ludewig, P.M., Phadke, V., Braman, J.P., Hassett, D.R., Cieminski, C.J., LaPrade, R.F., 2009. Motion of the shoulder complex during multiplanar humeral elevation. J. Bone Joint Surg.-Am. 91, 378–389. https://doi.org/10.2106/JBJS.G.01483.
Matsuki, K., Matsuki, K.O., Mu, S., Kenmoku, T., Yamaguchi, S., Ochiai, N., Sasho, T., Sugaya, H., Toyone, T., Wada, Y., Takahashi, K., Banks, S.A., 2014. In vivo 3D analysis of clavicular kinematics during scapular plane abduction: Comparison of dominant and non-dominant shoulders. Gait. Posture 39, 625–627. https://doi.org/10.1016/j.gaitpost.2013.06.021.
Matsuki, K., Matsuki, K.O., Mu, S., Yamaguchi, S., Ochiai, N., Sasho, T., Sugaya, H., Toyone, T., Wada, Y., Takahashi, K., Banks, S.A., 2011. In vivo 3-dimensional analysis of scapular kinematics: comparison of dominant and nondominant shoulders. J. Shoulder. Elbow. Surg. 20, 659–665. https://doi.org/10.1016/j.jse.2010.09.012.
Matsuki, K., Matsuki, K.O., Yamaguchi, S., Ochiai, N., Sasho, T., Sugaya, H., Toyone, T., Wada, Y., Takahashi, K., Banks, S.A., 2012. Dynamic In Vivo Glenohumeral Kinematics During Scapular Plane Abduction in Healthy Shoulders. J. Orthop. Sports. Phys. Ther. 42, 96–104. https://doi.org/10.2519/jospt.2012.3584.

Matsumura, N., Nakamichi, N., Ikegami, H., Nagura, T., Imanishi, N., Aiso, S., Toyama, Y., 2013. The function of the clavicle on scapular motion: a cadaveric study. J. Shoulder. Elbow. Surg. 22, 333–339. https://doi.org/10.1016/j.jse.2012.02.006.

McClure, P.W., Michener, L.A., Karduna, A.R., 2006. Shoulder Function and 3-Dimensional Scapular Kinematics in People With and Without Shoulder Impingement Syndrome. Phys. Ther. 86, 1075–1090. https://doi.org/10.1093/ptj/86.8.1075.

McClure, P.W., Michener, L.A., Sennett, B.J., Karduna, A.R., 2001. Direct 3-dimensional measurement of scapular kinematics during dynamic movements in vivo. J. Shoulder. Elbow. Surg. 10, 269–277. https://doi.org/10.1067/mse.2001.112954.

Michaud, B., Jackson, M.I., Prince, F., Begon, M.S., 2014. Can one angle be simply subtracted from another to determine range of motion in three-dimensional motion analysis? Comput. Methods. Biomech. Biomed. Eng. 17, 507–515. https://doi.org/10.1080/10255842.2012.696104.

Mitchell, M., Muftakhidinov, B., Winchen, T., Wilms, A., Schaik, B.V., Badshah400, Mo-Gul, Badger, T.G., Jędrzejewski-Szmek, Z., Kensington, Kylesower, 2020. markummitchell/engauge-digitizer: Nonrelease. Dataset, Zenodo. https://doi.org/10.5281/zenodo.597553.

Moher, D., Liberati, A., Tetzlaff, J., Altman, D.G., The PRISMA Group, 2009. Preferred Reporting Items for Systematic Reviews and Meta-Analyses: The PRISMA Statement. PLoS Med 6, e1000097. Doi: 10.1371/journal.pmed.1000097.

Moissenet, F., 2023. BLAB_Roboshoulder_dataset. Dataset, Zenodo. https://doi.org/10.5281/zenodo.8146966.

Moissenet, F., Feltrin, M., Rodriguez, P., Beaulieu, J.-Y., Holzer, N., 2023. A comprehensive dataset of ex vivo shoulder girdle kinematics during standardised humerus motions. Presented at the 11th ECCOMAS Thematic Conference on Multibody Dynamics, Lisbon, Portugal.

Moissenet, F., Puchaud, P., Naaïm, A., Holzer, N., Begon, M., 2025. Spartacus-shoulder-kinematics-dataset/shoulder-kinematics congress (0.3.1). Zenodo. https://doi.org/10.5281/zenodo.15161084.

Morrissey, D., Morrissey, M.C., Driver, W., King, J.B., Woledge, R.C., 2008. Manual landmark identification and tracking during the medial rotation test of the shoulder: An accuracy study using three-dimensional ultrasound and motion analysis measures. Man. Ther. 13, 529–535. https://doi.org/10.1016/j.math.2007.07.009.

Naaim, A., Moissenet, F., Duprey, S., Begon, M., Chèze, L., 2017. Effect of various upper limb multibody models on soft tissue artefact correction: A case study. J. Biomech. 62, 102–109. https://doi.org/10.1016/j.jbiomech.2017.01.031.

Nishikawa-Pacher, A., 2022. Research Questions with PICO: A Universal Mnemonic. Publications 10, 21. https://doi.org/10.3390/publications10030021.

Nishinaka, Naoya, et al., 2008. Determination of in vivo glenohumeral translation using fluoroscopy and shape-matching techniques. J. Shoulder Elbow Surg. 17 (2), 319–322. https://doi.org/10.1016/j.jse.2007.05.018.

Ohl, X., Lagacé, P.-Y., Billuart, F., Gagey, O., Skalli, W., Hagemeister, N., 2015. Robustness and Reproducibility of a Glenoid-centered Scapular Coordinate System Derived from Low-dose Stereoradiography Analysis. J. Appl. Biomech. 31, 56–61. https://doi.org/10.1123/JAB.2013-0310.

Oki, S., Matsumura, N., Iwamoto, W., Ikegami, H., Kiriyama, Y., Nakamura, T., Toyama, Y., Nagura, T., 2012. The Function of the Acromioclavicular and Coracoclavicular Ligaments in Shoulder Motion: A Whole-Cadaver Study. Am. J. Sports. Med 40, 2617–2626. https://doi.org/10.1177/0363546512458571.

Ortigas Vásquez, A., Taylor, W.R., Maas, A., Woiczinski, M., Grupp, T.M., Sauer, A., 2023. A frame orientation optimisation method for consistent interpretation of kinematic signals. Sci. Rep 13, 9632. https://doi.org/10.1038/s41598-023-36625-z.

Pain, L.A.M., Baker, R., Sohail, Q.Z., Richardson, D., Zabjek, K., Mogk, J.P.M., Agur, A.M. R., 2019. Three-dimensional assessment of the asymptomatic and post-stroke shoulder: intra-rater test–retest reliability and within-subject repeatability of the palpation and digitization approach. Disabil. Rehabil. 41, 1826–1834. https://doi.org/10.1080/09638288.2018.1451924.

Peeters, I., Braeckevelt, T., Herregodts, S., Palmans, T., De Wilde, L., Van Tongel, A., 2021. Kinematic Alterations in the Shoulder Complex in Rockwood V Acromioclavicular Injuries During Humerothoracic and Scapulothoracic Movements: A Whole-Cadaver Study. Am. J. Sports. Med 49, 3988–4000. https://doi.org/10.1177/03635465211053016.

Phadke, V., Braman, J.P., LaPrade, R.F., Ludewig, P.M., 2011. Comparison of glenohumeral motion using different rotation sequences. J. Biomech. 44, 700–705. https://doi.org/10.1016/j.jbiomech.2010.10.042.

Reid, D., Polson, K., Johnson, L., 2012. Acromioclavicular Joint Separations Grades I–III: A Review of the Literature and Development of Best Practice Guidelines. Sports. Med 42, 681–696. https://doi.org/10.1007/BF03262288.

Sahara, W., Sugamoto, K., Murai, M., Tanaka, H., Yoshikawa, H., 2006. 3D kinematic analysis of the acromioclavicular joint during arm abduction using vertically open MRI. J. Orthop. Res. 24, 1823–1831. https://doi.org/10.1002/jor.20208.

Sahara, W., Sugamoto, K., Murai, M., Yoshikawa, H., 2007. Three-dimensional clavicular and acromioclavicular rotations during arm abduction using vertically open MRI. J. Orthopaedic. Res. 25, 1243–1249. https://doi.org/10.1002/jor.20407.

Šenk, M., Chèze, L., 2006. Rotation sequence as an important factor in shoulder kinematics. Clin. Biomech. 21, S3–S8. https://doi.org/10.1016/j.clinbiomech.2005.09.007.

Seth, A., Matias, R., Veloso, A.P., Delp, S.L., 2016. A Biomechanical Model of the Scapulothoracic Joint to Accurately Capture Scapular Kinematics during Shoulder Movements. PLoS. One 11, e0141028. https://doi.org/10.1371/journal.pone.0141028.

Setliff, J.C., Anderst, W.J., 2024. A scoping review of human skeletal kinematics research using biplane radiography. J. Orthopaedic. Res. 42, 915–922. https://doi.org/10.1002/jor.25806.

Sugi, A., Matsuki, K., Fukushi, R., Shimoto, T., Hirose, T., Shibayama, Y., Nishinaka, N., Iba, K., Yamashita, T., Banks, S.A., 2021. Comparing in vivo three-dimensional shoulder elevation kinematics between standing and supine postures. JSES Int. 5, 1001–1007. https://doi.org/10.1016/j.jseint.2021.07.005.

Sulkar, Hema J., Zitnay, Jared L., Aliaj, Klevis, Henninger, Heath B., 2021. Proximal humeral coordinate systems can predict humerothoracic and glenohumeral kinematics of a full bone system. Gait & Posture 90, 380–387. https://doi.org/10.1016/j.gaitpost.2021.09.180. ISSN 0966-6362.

Teece, R.M., Lunden, J.B., Lloyd, A.S., Kaiser, A.P., Cieminski, C.J., Ludewig, P.M., 2008. Three-dimensional acromioclavicular joint motions during elevation of the arm. J. Orthop. Sports. Phys. Ther 38, 181–190. https://doi.org/10.2519/jospt.2008.2386.

Trinler, U., Baker, R., 2018. Estimated landmark calibration of biomechanical models for inverse kinematics. Med. Eng. Phys. 51, 79–83. https://doi.org/10.1016/j.medengphy.2017.10.015.

Ulman, S., Loewen, A., Erdman, A., Õunpuu, S., Chafetz, R., Tulchin-Francis, K., Wren, T. A.L., 2024. Model variations for tracking the trunk during sports testing in a motion capture lab. Front. Sports. Act. Living 6, 1429822. https://doi.org/10.3389/fspor.2024.1429822.

Van der Helm, F.C., 1997. A standardized protocol for motion recordings of the shoulder. Presented at the First conference of the international shoulder group, Citeseer, p. 12.

Vlachopoulos, L., Dünner, C., Gass, T., Graf, M., Goksel, O., Gerber, C., Székely, G., Fürnstahl, P., 2016. Computer algorithms for three-dimensional measurement of humeral anatomy: analysis of 140 paired humeri. J. Shoulder. Elbow. Surg. 25, e38–e48. https://doi.org/10.1016/j.jse.2015.07.027.

Von Eisenhart-Rothe, R., Matsen, F.A., Eckstein, F., Vogl, T., Graichen, H., 2005. Pathomechanics in atraumatic shoulder instability: scapular positioning correlates with humeral head centering. Clin. Orthopaedics Related Res. NA 82–89. https://doi.org/10.1097/01.blo.0000150338.27113.14.

Woltring, H.J., 1991. Representation and calculation of 3-D joint movement. Hum. Mov. Sci. 10, 603–616. https://doi.org/10.1016/0167-9457(91)90048-3.

Wu, G., Siegler, S., Allard, P., Kirtley, C., Leardini, A., Rosenbaum, D., Whittle, M., D'Lima, D.D., Cristofolini, L., Witte, H., Schmid, O., Stokes, I., 2002. ISB recommendation on definitions of joint coordinate system of various joints for the reporting of human joint motion—part I: ankle, hip, and spine. J. Biomech. 35, 543–548. https://doi.org/10.1016/S0021-9290(01)00222-6.

Wu, G., Van Der Helm, F.C.T., (DirkJan) Veeger, H.E.J., Makhsous, M., Van Roy, P., Anglin, C., Nagels, J., Karduna, A.R., McQuade, K., Wang, X., Werner, F.W., Buchholz, B., 2005. ISB recommendation on definitions of joint coordinate systems of various joints for the reporting of human joint motion—Part II: shoulder, elbow, wrist and hand. Journal of Biomechanics 38, 981–992. Doi: 10.1016/j.jbiomech.2004.05.042.

Yano, Y., Hamada, J., Tamai, K., Yoshizaki, K., Sahara, R., Fujiwara, T., Nohara, Y., 2010. Different scapular kinematics in healthy subjects during arm elevation and lowering: Glenohumeral and scapulothoracic patterns. J. Shoulder. Elbow. Surg. 19, 209–215. https://doi.org/10.1016/j.jse.2009.09.007.

Yoshida, Y., Matsumura, N., Miyamoto, A., Oki, S., Yokoyama, Y., Yamada, M., Yamada, Y., Nakamura, M., Nagura, T., Jinzaki, M., 2023. Three-dimensional shoulder kinematics: Upright four-dimensional computed tomography in comparison with an optical three-dimensional motion capture system. J. Orthopaedic. Res. 41, 196–205. https://doi.org/10.1002/jor.25342.